We are IntechOpen, the world's leading publisher of Open Access books Built by scientists, for scientists

4,800
Open access books available

122,000
International authors and editors

135M
Downloads

Our authors are among the

154
Countries delivered to

TOP 1%
most cited scientists

12.2%
Contributors from top 500 universities

CLARIVATE ANALYTICS BOOK CITATION INDEX INDEXED

WEB OF SCIENCE™

Selection of our books indexed in the Book Citation Index in Web of Science™ Core Collection (BKCI)

Interested in publishing with us?
Contact book.department@intechopen.com

Numbers displayed above are based on latest data collected.
For more information visit www.intechopen.com

10

Laser welding: techniques of real time sensing and control development

Xiaodong Na
Cummins Inc.
USA

1. Background

As shown in Figure 1, Laser Welding is a non-contact fusion process with various lasers applying to materials. Laser welding accomplishes the welding work through laser beam. With laser beam, energy is concentrated and used directly on the small welding area. Consequently, the welding zone is very narrow and hardly distorted due to little heat influence. Compared to traditional processes, Laser Welding is of potential. Its non-contact, localized, and narrow heat zone can create high quality result. Common re-working and after-work procedure are no more required, which saves cost and labour. Till now, Laser welding as been widely applied in various fields including automotive, microelectronics, aerospace, etc.

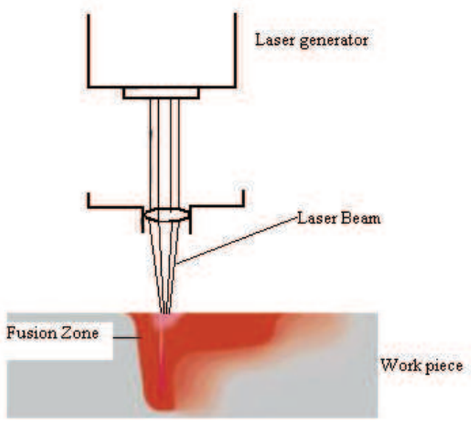

Fig. 1. Simple laser welding process

Common types of lasers applied to welding include CO2 gas laser, Solid state laser (YAG type), and Diode laser welding. CO2 laser uses a mixture of high purity carbon dioxide with helium and nitrogen as the medium, infrared of 10.6 micro-meters. Argon or helium is additionally used to prevent oxidation. YAG laser takes advantage of a solid bar of yttrium aluminium garnet doped with neodymium as the medium, whose infrared is only 1.06 micro-meters. Diode laser is mostly based on the conversion between high electrical to optical powers (Migliore 1998, Sun 1999, Sun 2002, Pedrotti 1993, Williams 1997).

Despite the quality performance in Laser Welding, the going concerns centres on any possible compromise of human and environmental health and safety. Indeed, these considerations have been challenging engineers to develop advanced automatic manufacturing process without any need of human involvements. However, successful development of automation system is beyond challenging because first of all, no exact model has been developed to describe the process and even it does, the model is much more complicate for control design; second of all, intelligent welding system requires appropriate and real time measurement working with specific developed control algorithm so that the process is robust and adaptive.
The major focus of this chapter will be on the real time sensing and control methods to the laser welding such that a practical automation system can be developed and implemented for heavy manufacturing and industry.

2. Overview of Laser Welding

Laser welding is an advanced fusion joining process that applies the energy converted from a laser beam to melt and joint metal pieces together. Laser beams can be either continuous or pulsed. Continuous laser systems are mostly used for very deep welding, whereas pulse lasers are used to weld very thin materials together. Depending on how the laser light is generated, Laser can be categorized into solid state lasers and gas lasers. Solid state lasers use solid media, such as synthetic ruby and crystal, to form the laser beam, such as Nd:YAG laser and Diode laser. Gas lasers use gaseous media, such as helium, nitrogen and carbon dioxide to form the laser beam, such as CO2 laser. Solid state lasers operate on much shorter wavelength than gas lasers, but they have much lower power outputs.
As shown in Figure 2, the advantage of laser welding is remarkable, e.g. low distortion, high speed and small heat affected zone. This is mostly because laser welding is applying a beam of light that is monochromatic, collimated and of sufficient power density. With adjustment power density, very high values of irradiance and much localized heating can be easily achieved. Because the light is collimated and monochromatic, the heat-affected zone can be very small without need of post processing, especially in the case of spot welding with extremely small weld diameter. System set up and configuration is also relatively easier and there is no contact of any material with the work piece. The disadvantage of laser welding is its cost and possibly limited capability. The initial capital cost of laser machine is usually very high. Depending on the laser system capacity, the depth of penetration in laser welding is also limited. Careful process monitoring and control is also required to avoid material vaporization due to high temperature around the weld.

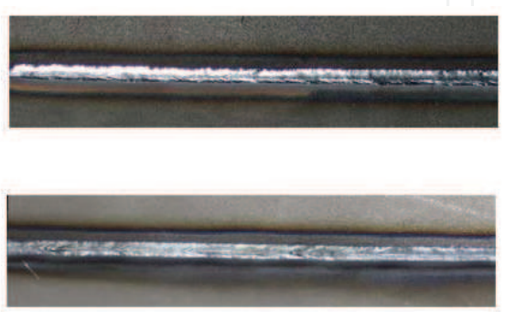

Fig. 2. Standard diode laser (1KW) welding results (9.5mm/s), 1.5mm thickness steel

By far Laser welding has been benefiting as many industries as possible from its advantages. Its applications vary with power-generation capability. Low-power applications are mostly seen in the instrumentation and electronics industries, while higher-power applications exist in the automotive, shipbuilding and aerospace industries. One potential disadvantage limiting its application is the cost, the more power of the laser provides, the higher cost it requires. For each application, the trade-off always involves with the capital cost of laser systems and the future economic returns.

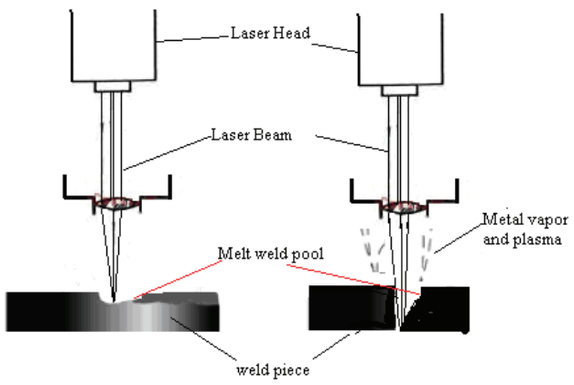

Fig. 3a. Conductivity based Laser Welding; 3b: Penetration based Laser Welding

Figure 3 presents standard system configuration for laser welding. As introduced earlier, fundamentally laser welding is through heat distribution process. Accordingly any factors that affect the laser power, welding speed and material complexity can impact the whole melting and jointing process. As shown in Figure 3a, heat distribution has the most significant impacts on the welding performance. For a laser with low power density, mostly heat converted from optical energy is completed through a conductive distribution. When laser power density is as big as KW level, heating the spot after laser focus transferred to the surface can boil and even vaporize the metal; accordingly a hole can be formed and filled with ionized metallic gas. The hole is also frequently referred as key-hole. The advantage of the cylindrical keyhole is that with key-hole formation, more effective heat energy will be absorbed and significantly boost welding process, especially by penetration, as shown in Fig. 3b. As a result, not only is the welding speed going to be much faster, but also the weld seam depth to width ratio much bigger. In addition, the heat-affected-zone can be relatively smaller, which is the most critical factor to welding quality.

3. Importance of Welding Automation

As introduced above, although laser welding highly advantageous, its process is potentially hazardous. For example, because of the heat and melting, particular fume, toxic noises and irradiation will be generated and exhausted to the working environment. Although with special care and human maintenance, these hazards can be reduced significantly, the risk of human error to some extent exposes operators and those around them to latent risks. Accordingly, it is always necessary to develop automatic control laser welding processes with limited or even without any need of human interference. Automation as a result offers a means of removing the operator from the process, reducing application-related hazards,

and more importantly improving the control of the welding environment. This is particularly beneficial for those heavy-duty manufacturing systems.

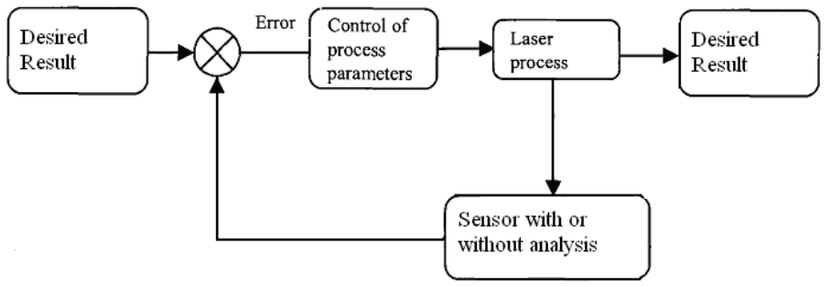

Fig. 4. standard automatic control laser welding process

Figure 4 represents a standard automatic laser welding process. Certainly any successful automation requires suitable sensor system for process signal acquisition and processing and practical control development for self adjustment. This way, control development and sensing system can constitute complete close-loop automation and intelligently make possible corrections online based on the current system state. For example, increase laser power when it is low; decrease travelling speed when it is high. The problem is that to perform online adjustment in general requires sufficient knowing knowledge about how the welding conditions such as laser power and speed impact the welding performance, i.e. weld pool geometry. In other words, the difficulty is how to implement a suitable relation to evaluate the process. Apparently successful control of the power and the speed during the welding process is the most significant step for the automation implementation. Since laser welding takes advantage of the heat energy to melt and joint the weld pieces, critical parameters that impact the energy should be taken care of at first. Power and travel speed are always considered the influential factors before designing laser welding automation. An easiest way is, taking the power and travel speed as input, the welding quality parameter as output, laser welding process could be achieved as a tracking control.

4. Real time sensing: a prerequisite for automation

As shown in Fig. 4, sensor system acquires and processes signals regarding the welding process such that any successful decision can be made, without which automation can not be complete. Sensing system development proves necessary to reduce any impacts on human health, detect any weld detect in real time and reduce overall operational cost, although it can be challenging because laser welding is dynamic, complex and uncertain. When the focused laser beam is applied to a material piece, spot of surface will be melted and around the fusion zone, energy is emitted in various forms. Each signal might carry information describing the characteristics of laser welding process. Figure 5 shows a selection of detectable emissions, such as optical, acoustic, infrared, vibration, and so on. Because of the significance of penetration, most of the sensing system is aimed at detecting either in-complete or over-penetration. In addition, the geometrical parameters of the keyhole and melt pool to some extent represent the welding quality. Accordingly analysis based on these measurable signals can help understand characteristics of the welding

process. So far, various studies have been done to monitor the laser welding process. Some focused on the emission signals such as acoustic, infrared, ultraviolet, plasma, and so on (Shao 2005, Ostendorf 2003, Ono 1992, Li 2002, Farson 1999, Steen 1986, Gu 1996). Others aimed to the weld pool images acquired with CCD cameras (Beersiek 2001, Zhang 1996, Na 2009, Beersiek 1999).

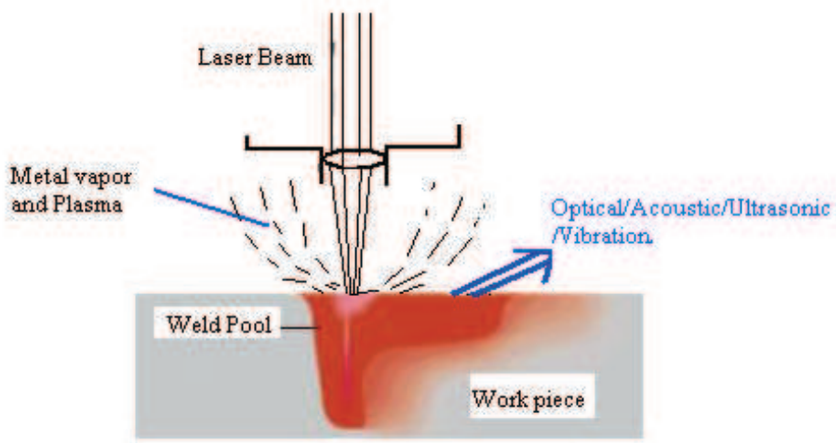

Fig. 5. Signal emissions and sensors in laser welding

5. Acoustic Signal sensing system

A lot of studies have been made on acoustic sensing for laser welding process (Sun 2002, Shao 2005, Ostendorf 2003, Ono 1992, Li 2002, Farson 1999, Steen 1986, Gu 1996). Others aimed to the weld pool images acquired with CCD cameras (Beersiek 2001, Zhang 1996, Na 2009, Beersiek 1999). Though it is promising, its application might be compromised by the complexity and noises in the laser welding. As shown in Fig. 6, in general the sensor is used to convert the measured sounds (e.g. weld pool surface) into electrical variable. The signal frequency can be up to 1MHz, from the human audible to ultrasonic range.

Because a normal audible signal falls into the range of 20Hz to 20 kHz, to monitor acoustic signal variation, a regular microphone can be used in applications. As presented in (Shao 2005, Farson 1999) it is quite possible to take advantage of micro-phone acquired acoustic signal to correlate the acoustic signal and welding performance. For example, spectrum analysis could indicate welding progress by analyzing any spike like fluctuations. A model was built describing the spectrum characteristics of the weld pool under various conditions. It has been demonstrated that there is a possible relation between key-hole oscillation and the frequency (Kroos 1993)

Ultrasonic signals were specifically investigated in search of a pattern or relationship describing the emission and the welding performance, e.g. weld pool geometry. A piezoelectric sensor is installed on the back of laser beam to capture any acoustic mirror signal generated by the back-reflected laser signal (Li 2002). Doing so was considering the dynamic vibration of the weld pool surface cause fluctuation of the reflected laser beam during welding process. It has been demonstrated that the signal strength varies with the distance from the weld pool. Moreover, in the case of deep penetration, i.e. generating a key-hole, a signal spike was noticed whenever key-hole was about to complete. Similar results were also shown in (Steen 1986) . In a study presented in (Gu 1996), FFT (Fast Fourier

Transform) was applied to obtain the frequency response between 20 kHz and 0.5 MHz to investigate resonant relationship during last welding. It has been proved that with manipulating frequency components, it was possible to isolate welding process from over-penetration or partial penetration. Similar studies are also described in (Miller 2002, Klein 2002)

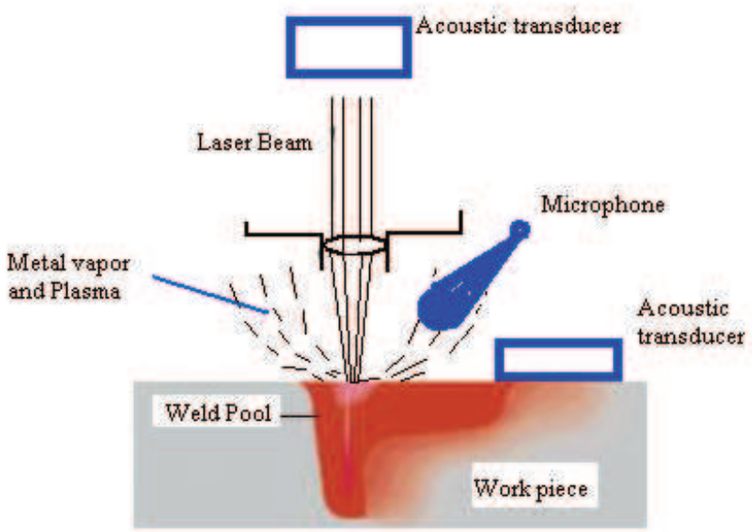

Fig. 6. Acoustic sensing system set up

With aid of acoustic emission signal analysis, reliable and applicable measurement and control of laser welding becomes possible. The disadvantage of these methods is its limit while differentiate from partial penetration and full penetration. The sensing system is also very easily influenced by instable noise.

6. Optical Signal sensing system

As shown in Figure 7, Optical sensor is mostly based on the detection of plasma plume emission and the thermal radiation of the weld pool. Fundamentally this is considering the associative relation between the degree of penetration and the emission intensity measurement. Various studies have been done on optical signal sensor design (Ostendorf 2004, Tonshoff 1998, Park 1999, Park 2002, Sforza 2002). In (Tonshoff 1998), a silicon photodiode assisted with a preamplifier is developed to detect dynamic plasma intensity fluctuation during laser welding. Similar study is also done in (Park 2002) based on Ultra-violet photodiodes and Infrared photodiode to measure the emission from the plasma and metal vapor in the CO2 laser welding searching for a relationship describing the heat distribution and the emissions. A pattern to correlate the laser energy under conditions such as optimal heat input, slightly low heat input and low heat input with welding quality such as complete and partial joining is also developed. Similar experiments were implemented in (Park 1999, Park 2002) to develop a relationship between the plasma and spatter and bead shape according to the welding variables, based on a multiple regression analysis and neural network to estimate the penetration depth and width of the weld bead. In (Sforza

2002, Zhang 2004), IR and UV signals were captured and analyzed to detect the IR and UV waveband of the optical emissions induced in the underwater laser welding and searched for a relationship between the optical signals and the weld quality with various shielding conditions.

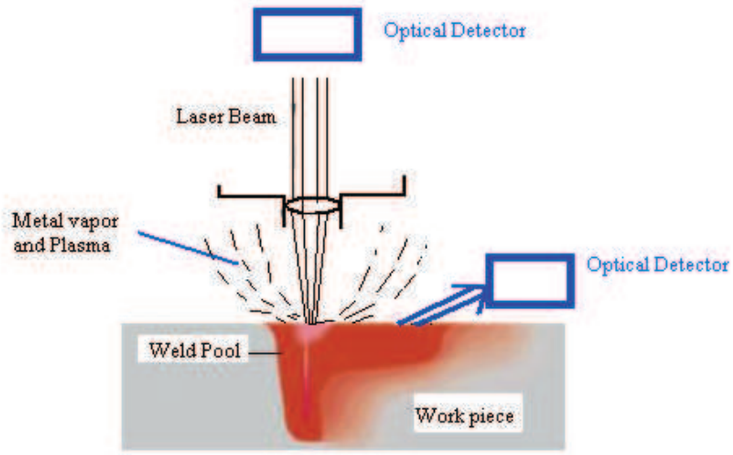

Fig. 7. Optical Signal Sensors

Similar to those acoustic sensing system, optical sensor is easier to implement and of low cost. However, its accuracy is compromised by the system noises.

7. Vision based Keyhole Sensing with CCD/CMOS Camera

During the process of laser welding, high energy of laser beam is focused onto a single location and a keyhole is created. As shown in Figure 8, to ensure successful welding and avoid effects like burnt-through, keyhole depth should be controlled not too much beyond the height of the material. The advantage of Keyhole sensing is the possible small heated zone, which results in better after-work quality.

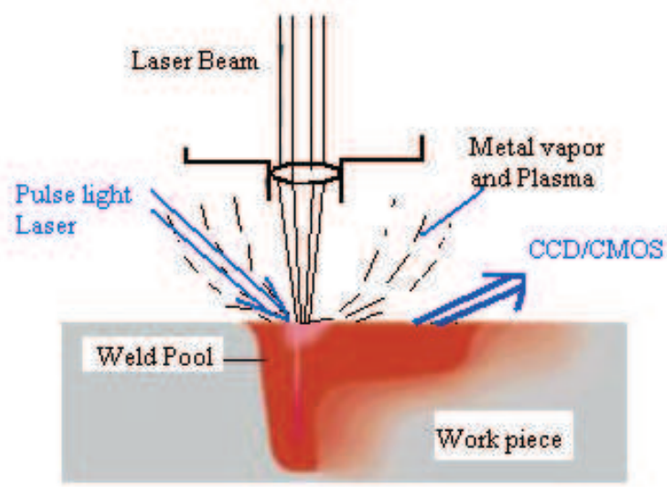

Fig. 8. Vision Sensor

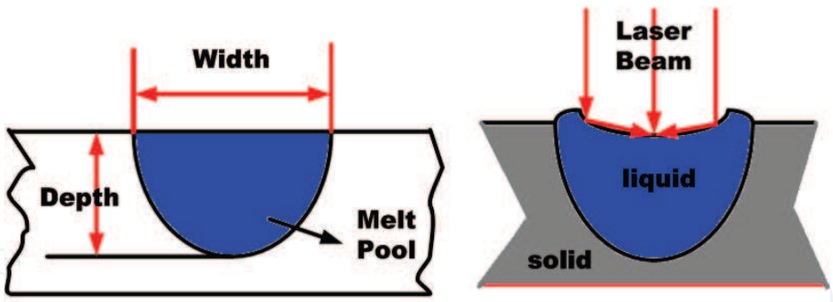

Fig. 9. Weld pool (1a) Laser Welding (1b)

As shown in Figure 9, the full knowledge of the weld pool geometry includes the length, the width, and the depth. Weld pool images were acquired with CCD/CMOS cameras and studied to investigate the relations among various parameters along with laser welding process. Various Researches has been done related to welding pool measurement based on the vision sensing tool such as monochrome camera and optic sensors. Through the sensors, welding related information is achieved online or offline so that control loop can adjust the welding process parameters. Considering the role of penetration to welding process, many study started with penetration measurement and control. Successful 2D or 3D measurement can provide sufficient geometric weld pool information and consequently the control performance (Farson 1999, Lankalpall 1996, Becker 1995). In 0, a camera system was developed to measure the surface geometric size of the weld pool. In (Na 2009, Zhang 1996,Beersiek 2000), a system for process monitoring of laser beam welding based on a CMOS-camera was presented. The system observed the welding process online and coaxial to the laser beam. It was used to investigate the geometrical parameters of the keyhole.

8. Other sensing techniques

Besides acoustic and optical signals, temperature distribution can also be examined. In (Jeon 1998), the surface temperature variation in the laser brazing of a pin-to-hole joint is studied using an infrared radiation sensor. In (Bertrand 2000), surface temperature in Nd:YAG continuous laser welding is monitored to identify the variation of brightness temperature whenever certain welding defects occur. In (Lim 1998) an infrared sensor is used to study laser spot welding. In (Li 1996) a special plasma charge sensor (PCS) based on plasma density and ionization variation is implemented to measure weld penetration and detect weld defects. Some other researches are also involved with direct mode estimation (Morgan 1990, Sun 1993) to assist better control development.

9. Vision sensor based system identification and control

Figure 10 presents a standard diode laser welding system, developed in the Welding Research Lab at the University of Kentucky. The laser is current-driven and the output energy is theoretically proportional to its input current. According to the manufacturing configuration, the wavelength of the laser light is 850nm and the power can reach to 1 $\mathrm{k}W$ at most, which corresponds to the current at the level of 58mA. The workstation

holding the work-piece is driven by a servo motor. Both the driving current of the laser and the welding speed are controlled by a digital computer. In addition, there are two other parameters, namely the laser focus distance and incident angle. For simplification purposes, the authors adjusted the laser focus distance and incident angle at 89mm and 42 degree respectively according to manufacturing settings. As shown in Figure 11, the vision sensor measures the top surface width for model identification and control design. A close seam tracking is finally possible.

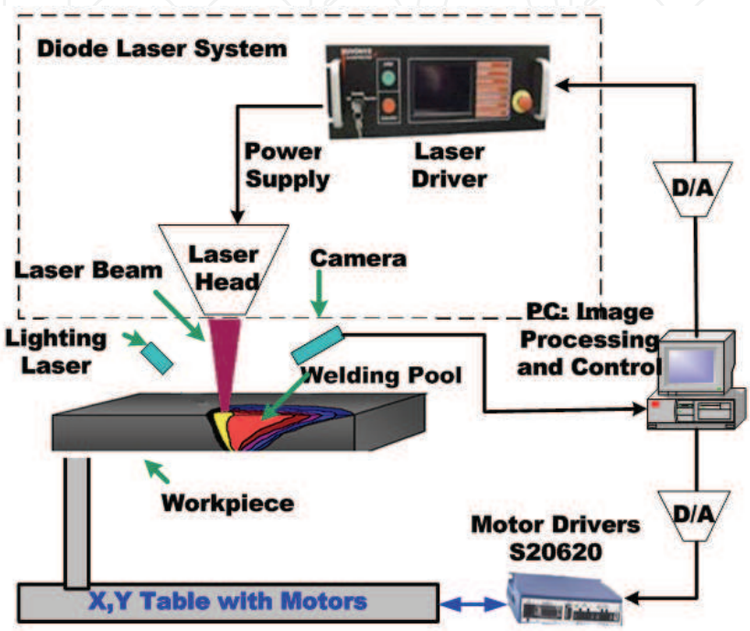

Fig. 10. Standard vision sensor based automatic diode laser welding system

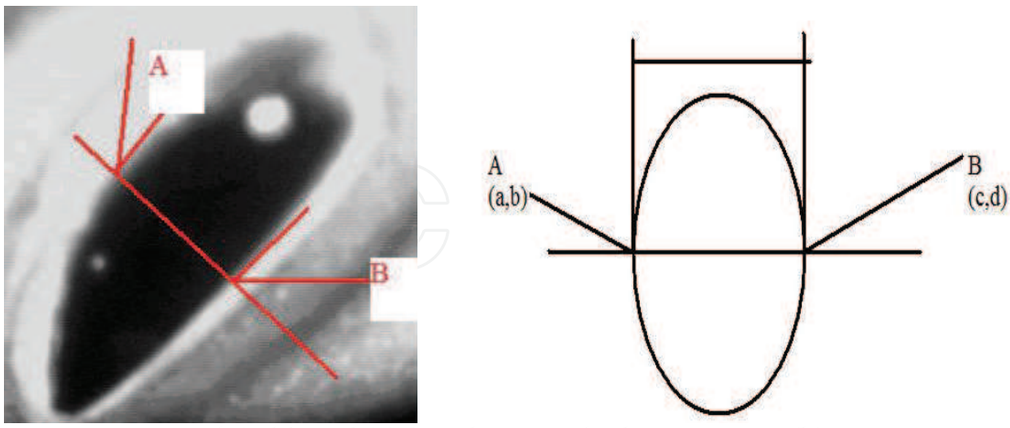

Fig. 11. raw picture of Weld pool (a) Simple view of Edge Detection (b)

10. Nonlinear Hammerstein identification (Na 2009)

As introduced above, Laser welding is a complicated thermodynamic and physicochemical process, which involves material melting, evaporating, plasma forming, keyhole occurrence

and so on. The weld shape is determined by many parameters in the thermodynamic and physicochemical process, such as the relative speed between the laser and the work-piece. Thus, the laser welding should be treated as a nonlinear process. Traditionally, a linear model is often used to approximate a nonlinear system. However, the linear model can only describe the local dynamics in the vicinity of the set point and the control system designed by using the linear approximated model has small operation region. To understand/describe the global behavior of the laser welding process and to obtain a large operation region for the control system, a nonlinear model is preferred. However, the process is so complicated that it is hardly possible to build the model solely through physicochemical analysis. Therefore, nonlinear identification, which is based on input-output data, is needed.

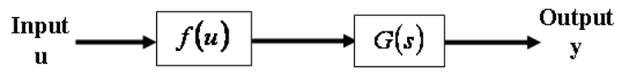

Fig. 12. Continuous Hammerstein structure

Figure 12 is the continuous Hammerstein structure used for identifying a practical model to the laser welding process. The structure consists of nonlinearity in series with a linear dynamics, where u and y are the input and the output respectively. The linear dynamics can in general be represented by a linear transfer function:

$$G(s)=\frac{b_0 s^m + b_1 s^{m-1} + \cdots + b_m}{a_0 s^n + a_1 s^{n-1} + \cdots + a_n} = \frac{B(s)}{A(s)}, \tag{1}$$

where $\{a_i\}, i = 0,1,\cdots n$ and $\{b_i\}, i = 0,1,\cdots m$ are parameters of the linear dynamics; and the nonlinearity $f(u(t))$ can be considered as a nonlinear function of the system input and the input of the linear dynamics. Further, as will be seen later, the linear dynamics of the diode laser process can be sufficiently approximated without zeros, in other words, a class of nonlinear dynamic systems whose linear dynamics is of minimum phase.
Then in the Laplace domain:

$$y(s) = G(s)L(f(u(t))), \tag{2}$$

where L is the operator of Laplace transform.
Without loss of generality, denote

$$a_n = 1 \tag{3}$$

$$K(u(t)) = L^{-1}(B(s)L(f(u(t)))), \tag{4}$$

where L^{-1} is the operator of inverse Laplace transform.
Then with substitution, (2) can be rewritten as:

$$a_0 y^{(n)}(t) + a_1 y^{(n-1)}(t) + \cdots y(t) = K(u(t)) \tag{5}$$

Rewrite (5) into matrix form:

$$y(t) = \phi^T(t)\theta \tag{6}$$

$$\phi^T(t) = \left[-y^{(n)}(t) \quad \cdots \quad -y^{(1)}(t) \quad 1\right] \tag{7}$$

$$\theta^T = \left[a_0 \quad \cdots \quad a_{n-1} \quad K(u(t))\right] \tag{8}$$

Accordingly this Nonlinear Hammerstein identification becomes to estimate unknown parameters in (8). Among these parameters only $K(u(t))$ will vary with the inputs.
Suppose $f(u(t))$ is a polynomial:

$$f(u(t)) = C_0 + C_1 u(t) + \cdots + C_p u^p(t); \tag{9}$$

And further consider step input $u(t) = U$ in Fig. 7. Therefore, $f(u(t))$ is also a step signal whose Laplace transform can be obtained by $L(f(u(t))) = f(U)/s$; therefore, the linear dynamics (1) can be simplified to:

$$G(s) = \frac{b_m}{a_0 s^n + a_1 s^{n-1} + \cdots + 1} \tag{10}$$

Furthermore, the system can be can be simplified as:

$$a_0 y^{(n)}(t) + a_1 y^{(n-1)}(t) + \cdots y(t) = K(u(t)) \tag{11}$$

where

$$K(u) = b_m f(U) \tag{12}$$

and b_m is a constant.
As a result, the proposed identification for a specific Hammerstein structure with (10) as the linear dynamics and (12) as the nonlinear static function in general can be achieved in two steps:
Step 1: Identify A(s) under different step input $\{U_j\}, j = 1, \cdots, M$ (13)
Due to the use of a step input U_j, the nonlinearity function,

$$K(u) = K(U_j) = b_m f(U_j), \tag{14}$$

becomes a constant parameter and can be identified by:

$$\theta^T(U_j) = \left[a_0 \quad \cdots \quad a_{n-1} \quad K(U_j)\right]. \tag{15}$$

Hence, both the format of A(s) and the value of $b_m f(U_j)$ can be identified.

Step 2: Determine the nonlinear function $f(u)$ and b_m from the steady-state responses $Y(U_j)$ under step inputs, $\{U_j\}, j = 1, \cdots, M$.

In this case, the nonlinearity function can be identified by:

$$K(U_j) = \phi^T(U_j)\theta, \tag{16}$$

where
$$\phi^T(U_j) = \begin{bmatrix} 1 & U_j & U_j^2 & \cdots & U_j^p \end{bmatrix} \tag{17}$$

and
$$\theta^T = \begin{bmatrix} b_m C_0 & b_m C_1 & b_m C_2 & \cdots & b_m C^p \end{bmatrix}. \tag{18}$$

Then the parameters in $b_m f(U_j)$ can be estimated by such as linear least square algorithm:

$$\theta = (\Phi^T \Phi)^{-1} \Phi^T \begin{bmatrix} Y(U_1) & \cdots & Y(U_M) \end{bmatrix}^T \tag{19}$$

where $\Phi^T = \begin{bmatrix} \phi^T(U_1) & \cdots & \phi^T(U_M) \end{bmatrix}^T$.

11. Nonlinear Constructive Control Design (Liu 2002, Liu, 2003, Liu 2004)

We consider the system that can be represented by:

$$y^n(y) = f(y, \dot{y}, \cdots, y^{n-1}) + \theta u + g(u) \tag{20},$$

where y, u are the output and the control respectively; $y^i, i = 1,2, \cdots n$ is the ith derivative of y; and $f(y, \dot{y}, \cdots, y^{n-1}) \le \theta \bar{f}(y, \dot{y}, \cdots, y^{n-1})$, where $\theta > 0$

$g(u) \le c\|g(u)\|$, where $c > 0$

$x_1 = y$

$\cdots$

Let $x_n = y^{n-1}$, where v is the virtual control input for the system

$v = u$

$z = v$

Then we have:

$$\begin{aligned} \dot{x}_i &= x_{i+1} \\ \dot{x}_n &= f(x) + u, \\ 1 &\le i \le n-1 \end{aligned} \tag{21}$$

where $x = \begin{bmatrix} x_1 & x_2 & \cdots & x_n \end{bmatrix}^T$

During the identification, $g(u)$ is approximated by a polynomial. In fact, it can be other complex formats. However, we assume that $g(u)$ is continuous and bounded

We further assume all the states of the system are available for feedback and define:

$$\begin{aligned} e_1 &= x_1 - x_d \\ &\cdots \\ e_{n-1} &= x_n - x_d^{n-2} \\ e_n &= x_n - x_d^{n-1} \end{aligned} \tag{22}$$

With simple substitution, we can have:

$$\begin{aligned} \dot{e} &= Ae + b\left(f\left(e+\bar{x}_d, z\right) + \theta v - x_d^{n} + g\left(e+\bar{x}_d\right)\right) \\ z &= v \end{aligned} \tag{23},$$

where $A = \begin{bmatrix} 0 & 1 & 0 & 0 \\ \vdots & \vdots & \vdots & \vdots \\ 0 & 0 & 0 & 1 \\ 0 & 0 & 0 & 0 \end{bmatrix}$, $b = \begin{bmatrix} 0 \\ \vdots \\ 0 \\ 1 \end{bmatrix}$, and $\bar{x}_d = \begin{bmatrix} x_d & \cdots & x_d^{n-1} & x_d^{n} \end{bmatrix}$.

Define $A_m = A - bK$, where K is chosen so that the matrix $A_m = A - bK$ is Hurwitz. Then,

$$\begin{aligned} \dot{e} &= A_m e + b\left(f\left(e+\bar{x}_d, z\right) + \theta v - x_d^{n} + g\left(e+\bar{x}_d\right)\right) \\ z &= v \end{aligned} \tag{24}$$

Further, we define a dynamic signal described by:

$$\begin{aligned} \dot{r} &= -c_0 r + r_m\left(e, \bar{x}_d\right) \\ r(0) &> 0 \\ c_0 &> 0 \\ r_m &= \left\|e+\bar{x}_d\right\|^2 \gamma_0 \left\|e+\bar{x}_d\right\| + d_0 \end{aligned} \tag{25}$$

From [40], signal r has the property of :

$$V \le r(t) + D(t) \tag{26}$$

Then the robust adaptive controller can be designed by:

$$\begin{aligned} v &= -\beta e^T P b\left(\bar{f}\left(e+\bar{x}_d, z\right) + \left\|e+\bar{x}_d\right\|^2 + \|z\|^2 + \left(\alpha^{-1}(2r)\right)^2 + (Ke)^2 + 1\right) \\ \dot{\beta} &= \beta_m\left(e, z, r, \bar{x}_d\right) - \Gamma\sigma\beta \\ \beta_m &= \Gamma\left(e^T P b\right)^2\left(\bar{f}\left(e+\bar{x}_d, z\right) + \left\|e+\bar{x}_d\right\|^2 + \|z\|^2 + \left(\alpha^{-1}(2r)\right)^2 + (Ke)^2 + 1\right) \\ \Gamma &> 0 \\ \sigma &> 0 \end{aligned} \tag{27}$$

$\alpha^{-1}(\bullet)$ is the inverse of function of $\alpha(\bullet)$ and P is the solution of

$$\begin{aligned} &PA_m + A_m{}^T = -Q \\ &Q = Q^T > 0 \end{aligned} \tag{28}$$

Define the Lyapunov candidate as:

$V = e^T Pe + \theta\Gamma^{-1}\left(\beta - \hat{\beta}\right)^2$, where $\hat{\beta}$ is a positive constant and the desired value of β

$$\begin{aligned} \dot{V} &= -\left(A_m e + b\left(f\left(e+\bar{x}_d, z\right) + \theta v - x_d{}^n + g\left(e+\bar{x}_d\right)\right)\right)^T Pe + e^T P\left(A_m e + b\left(f\left(e+\bar{x}_d, z\right) + \theta v - x_d{}^n + g\left(e+\bar{x}_d\right)\right)\right) + V_1 \\ &\le -e^T Qe + 2\bar{\beta}\theta\left(\left(e^T Pb\right)(Ke) - \frac{1}{2\hat{\beta}\theta}\right)^2 - 2\bar{\beta}\theta\left(\left(e^T Pb\right)\bar{f}\left(e+\bar{x}_d, z\right) - \frac{\theta}{2\hat{\beta}\theta}\right)^2 + \frac{\theta^2}{2\hat{\beta}\theta} - 2\bar{\beta}\theta\left(\left(e^T Pb\right)\left(e+\bar{x}_d\right) - \frac{c_1}{2\hat{\beta}\theta}\right)^2 \\ &+ \frac{c_1{}^2}{2\hat{\beta}\theta} - 2\bar{\beta}\theta\left(\left(e^T Pb\right)(z) - \frac{c_2}{2\hat{\beta}\theta}\right)^2 + \frac{c_2{}^2}{2\hat{\beta}\theta} - 2\bar{\beta}\theta\left(\left(e^T Pb\right)\left(\alpha^{-1}(2r)\right) - \frac{c_3}{2\hat{\beta}\theta}\right)^2 + \frac{c_3{}^2}{2\hat{\beta}\theta} - 2\bar{\beta}\theta\left(\left(e^T Pb\right) - \frac{c_4}{2\hat{\beta}\theta}\right)^2 \\ &+ \frac{c_4{}^2}{2\hat{\beta}\theta} - \theta\sigma\beta^2 + \theta\sigma\hat{\beta}^2 - \theta\sigma\left(\beta - \hat{\beta}\right)^2 \end{aligned} \tag{29}$$

where,

$$V_1 = 2\theta\Gamma^{-1}\left(\beta - \hat{\beta}\right)\left(\Gamma\left(e^T Pb\right)^2\left(\bar{f}\left(e+\bar{x}_d, z\right) + \left\|e+\bar{x}_d\right\|^2 + \|z\|^2 + \left(\alpha^{-1}(2r)\right)^2 + (Ke)^2 + 1\right) - \Gamma\sigma\beta\right)$$

$$c_4 = \sup\left(\left\|y_r{}^n\right\| + c_3\left\|g\left(e+\bar{x}_d\right)\right\| + \alpha^{-1}\left(D(t)\right)\right)$$

Accordingly,

$$\begin{aligned} &\dot{V} \le -e^T Qe - \theta\sigma\left(\beta - \hat{\beta}\right)^2 + M \\ &M = \frac{1}{2\beta\theta}\left(c_1{}^2 + c_2{}^2 + c_3{}^2 + c_4{}^2 + \theta^2 + 1\right) + \sigma\theta\hat{\beta}^2 \end{aligned} \tag{30}$$

As a result, the Lyapunov function V will decrease monotonically, which means that (e, β) are bounded. The system is accordingly bounded asymptotically stable

12. Related to the Diode Laser Processing System Without $\dot{u}$

As shown in the identification, our laser welding system can be represented by:

$$\begin{aligned} &\ddot{y}(t) = \theta_1 y + \theta_2 \dot{y}(t) + \theta_3 + \theta_4 u(t) + \theta_5 u^2(t) \\ &+ \theta_6 u^3(t) + \theta_7 u^4(t) \end{aligned} \tag{31}$$

Define the state function as:

$$\begin{aligned} x_1(t) &= y(t) \\ x_2(t) &= \dot{y}(t) \\ z(t) &= u(t) \\ z(t) &= v \end{aligned} \tag{32}$$

Then the system can be represented by:

$$\begin{aligned}\dot{x}_1(t) &= x_2(t)\\ \dot{x}_2(t) &= \theta_1 x_1(t) + \theta_2 x_2(t) + \theta_3 + \theta_4 z(t) + \theta_5 z^2(t) + \theta_6 z(t)^3 + \theta_7 z(t)^{\backslash 4} + \theta_8 v\end{aligned} \tag{33}$$

For simplicity, we let the nonlinear function be:

$$f(\cdot) = \theta_1 x_1(t) + \theta_2 x_2(t) + \theta_4 z(t) + \theta_5 z^2(t) + \theta_6 z(t)^3 + \theta_7 z(t)^4 \tag{34}$$

Accordingly, the amplitude limit function can be written as:

$$f(\cdot) \le \left\| \theta_1 x_1(t) + \theta_2 x_2(t) + \theta_4 z(t) + \theta_5 z^2(t) + \theta_6 z(t)^3 + \theta_7 z(t)^4 \right\| \tag{35}$$

$f(\cdot) \le \theta\left(\sqrt{x_1^{\,2}} + \sqrt{x_2^{\,2}} + \sqrt{z^2} + z^2 + \sqrt{z^6} \right)$, where θ can be unknown

Thus:

$$\bar{f}(\cdot) = \sqrt{x_1^{\,2}} + \sqrt{x_2^{\,2}} + \sqrt{z^2} + z^2 + \sqrt{z^6} \tag{36}$$

Equation 36 gives the boundary of the nonlinearity function.

Let the tracking signal $y_r = \sin(t)$, the standard sinusoidal signal with amplitude 1

Then the error signal can be written by:

$$\begin{aligned}e_1(t) &= x_1(t) - y_r(t)\\ e_2(t) &= x_2(t) - \dot{y}_r(t)\end{aligned} \tag{37}$$

or,

$$\begin{aligned}\dot{e}_1(t) &= e_2(t)\\ \dot{e}_2(t) &= \theta_1 + \theta_8 v + \theta_4 z + \theta_5 z^2 + \theta_6 z^3 + \theta_7 z^4 - \ddot{y}_r(t)\\ z(t) &= v\end{aligned} \tag{38}$$

or,

$$\dot{e}(t) = \begin{bmatrix} 0 & 1 \\ 0 & 0 \end{bmatrix} e + \begin{bmatrix} 0 \\ 1 \end{bmatrix} \left[f(e + y_r, z) - \ddot{y}_r(t) + \theta_5 v + \theta_3 \right] \tag{39}$$

let

$$\text{A} = \begin{bmatrix} 0 & 1 \\ 0 & 0 \end{bmatrix} \text{ and } b = \begin{bmatrix} 0 \\ 1 \end{bmatrix} \tag{40}$$

Then equation 9.3 can be rewritten by:

$$\dot{e}(t) = Ae + b\left[f(e + y_r, z) - \ddot{y}_r(t) + \theta_5 v + \theta_3 \right] \tag{41}$$

With simpler substitution, the error matrix is:

$$\dot{e}(t)=\begin{bmatrix}0 & 1\\ 0 & 0\end{bmatrix}e+\begin{bmatrix}0\\ 1\end{bmatrix}\left[f\left(e+y_r,z\right)-\ddot{y}_r(t)+\theta_5 v+\theta_3\right] \tag{42}$$

To design the controller, we reformat the equation as:

$$\dot{e}(t)=A_m e+b\left[Ke+f\left(e+y_r,z\right)-\ddot{y}_r(k-3)+\theta_5 v+\theta_3\right] \tag{43}$$

, where $A_m=A-bK$ and K is chosen so that A_m is Hurwitz.

$$\dot{e}(t)=\begin{bmatrix}0 & 1\\ -2 & -4\end{bmatrix}e+\begin{bmatrix}0\\ 1\end{bmatrix}\left[\begin{bmatrix}2 & 4\end{bmatrix}\begin{bmatrix}e_1\\ e_2\end{bmatrix}+f\left(e+y_r,z\right)-\ddot{y}_r(t)+\theta_5 v+\theta_3\right] \tag{44}$$

For matrix:

$$A_m=\begin{bmatrix}0 & 1\\ 0 & 0\end{bmatrix}-\begin{bmatrix}0\\ 1\end{bmatrix}\begin{bmatrix}k_1 & k_2\end{bmatrix} \tag{45}$$

$$A_m=\begin{bmatrix}0 & 1\\ -k_1 & -k_2\end{bmatrix} \tag{46}$$

The constant matrix $K=\begin{bmatrix}k_1 & k_2\end{bmatrix}$ is chosen so that the roots of the characteristic equation have negative real parts.
We then can design the robust adaptive controller

$$v=-\beta e^T Pb\left\{\left[f\left(e+y_r,z\right)\right]^2+\left\|e+y_r\right\|^2+\left\|z\right\|^2+\left[\alpha^{-1}(2r)\right]^2+(Ke)^2+1\right\}, \tag{47}$$

where β is the adaptive parameter of the controller and $\alpha_1{}^{-1}$ is the inverse function and is a function of class K_∞. For now, we assume $\alpha_1(\cdot)=\left\|\cdot\right\|^2$
P is Lyapunov matrix under the condition of:

$$PA_m+A_m{}^T=-Q, \text{ where } Q=Q^T>0 \tag{48}$$

$$\dot{\beta}=\beta_m\left(e,z,r,y_r\right)-\Gamma\sigma\beta \tag{49}$$

$$\beta_m=\Gamma\left(e^T Pb\right)^2\left\{\left[f\left(e+y_r,z\right)\right]^2+\left\|e+y_r\right\|^2+\left\|z\right\|^2+\left[\alpha^{-1}(2r)\right]^2+(Ke)^2+1\right\} \tag{50}$$

For the design constants we assume they are known and satisfy the condition of

$$T>0,\sigma>0 \tag{51}$$

Because in our experiments, only the position signal is detected, we further implement high gain observer for the purpose of output feedback.

Let the error signal be:

$$\begin{aligned}\dot{\hat{e}}_1 &= \hat{e}_2 + \left(\frac{\sigma_1}{\varepsilon}\right)\left(e_1 - \hat{e}_1\right),\\ \hat{e}_2 &= \left(\frac{\sigma_2}{\varepsilon^2}\right)\left(e_1 - \hat{e}_1\right)\end{aligned} \tag{52}$$

where $\varepsilon > 0$ is a small constant, $\sigma_i > 0, i = 1,2$ are chosen so that $A_n = A - K_\sigma C$ is a Hurwitz matrix, and

$$K_\sigma = \begin{bmatrix}\sigma_1 & \sigma_2\end{bmatrix},\ C = \begin{bmatrix}1 & 0\end{bmatrix} \tag{53}$$

Accordingly for the matrix:

$$A_n = \begin{bmatrix}0 & 1\\ 0 & 0\end{bmatrix} - \begin{bmatrix}\sigma_1 & \sigma_2\end{bmatrix}\begin{bmatrix}1\\ 0\end{bmatrix} \tag{54}$$

$$A_n = \begin{bmatrix}-\sigma_1 & 1\\ -\sigma_2 & 0\end{bmatrix} \tag{55}$$

The positive constants matrix $K_\sigma = \begin{bmatrix}\sigma_1 & \sigma_2\end{bmatrix}$ is chosen so that the characteristic equation $s^2 + \sigma_1 s + \sigma_2 = 0$ has the roots with negative real parts.
To eliminate peaking in the implementation of the observer, we define

$$\begin{aligned}\hat{e}_1 &= \frac{q_1}{\varepsilon}\\ \hat{e}_2 &= q_2\end{aligned} \tag{56}$$

Thus:

$$\begin{aligned}\varepsilon\dot{q}_1 &= q_2 + \sigma_1\left(e_1 - q_1\right)\\ \varepsilon\dot{q}_2 &= \sigma_2\left(e_1 - q_1\right)\end{aligned} \tag{57}$$

In order to prevent the peaking from entering the control system, we saturate the control signal and adaptive controller outside of their domains of interests. In our experiments,

$$\begin{aligned}M_v &= 50\\ M_\beta &= 30\end{aligned} \tag{58}$$

With these constants, which are larger than or equal to the upper bound of those signals $v\left(e, r, \bar{y}_r, \beta\right), \beta_m\left(e, r, \bar{y}_r\right)$, we can denote the following equations:

$$v^S\left(e, r, \bar{y}_r, \beta\right) = M_v sat\left(\frac{v\left(e, r, \bar{y}_r, \beta\right)}{M_v}\right) \tag{59}$$

$$\beta_m{}^S(e,r,\bar{y}_r) = M_\beta sat\left(\frac{\beta_m(e,r,\bar{y}_r)}{M_\beta}\right) \tag{60}$$

$$sat(\ ): \text{saturation function} \tag{61}$$

Thus the robust adaptive output controller can be obtained by replacing $v(e,r,\bar{y}_r,\beta)$ and $\beta_m(e,r,\bar{y}_r)$ with $v^S(e,r,\bar{y}_r,\beta)$ and $\beta_m{}^S(e,r,\bar{y}_r,\beta)$

Simulation results:

We choose the constants:

$$\sigma = 0.00001, K = \begin{bmatrix} 2 & 4 \end{bmatrix}, P = \begin{bmatrix} 1.375 & 0.25 \\ 0.25 & 0.1875 \end{bmatrix}, Q = \begin{bmatrix} 1 & 0 \\ 0 & 1 \end{bmatrix}.$$

The simulation track two different input signal respectively: Both simulations are tested with adding 0.5sin(t) as disturbance.

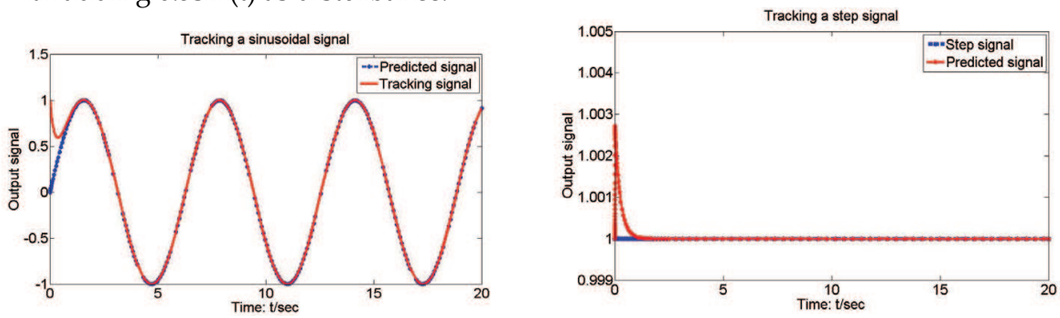

Fig. 13. Tracking sinusoidal and step signals

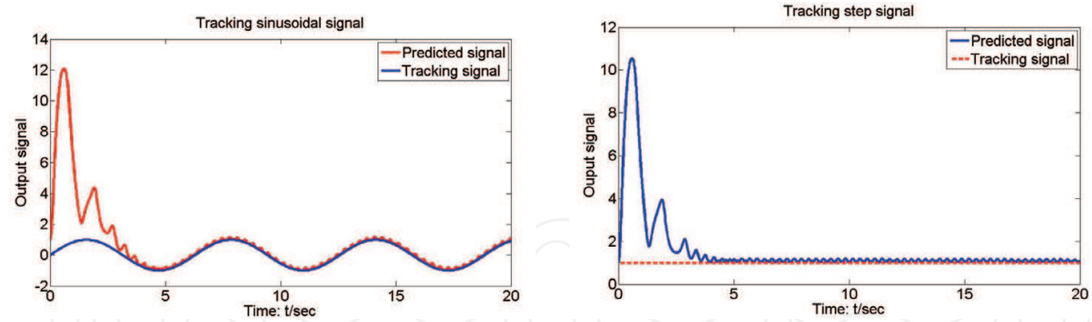

Fig. 14 Tracking step signal: Output feedback

Apparently the state feedback tracks better with either Sinusoidal or Step signal although he observer design somewhat caused a fluctuation with very small amplitude. This might require further tuning on the constants

13. References

Beersiek, J. (1999), On-line monitoring of keyhole instabilities during laser beam welding, ICALEO (R) 99: Section D, 49-58

Beersiek, J. (2000), "A CMOS Camera as a Tool for Process Analysis Not Only for Laser Beam," ICALEO'01 92&93: 1185-1193, 2000

Beersiek, J. (2001), "A CMOS camera as a tool for process analysis not only for laser beam welding," 20th ICALEO Vols 92&93, 1185-1193, 2001

Becker, S. and. Beersiek, J. (2000), "Semi-Automatic 3D Model Extraction from Uncalibrated 2D Camera Views," SPIE Visual Data Exploration and Analysis II 2410: 447-461, 1995

Bertrand, P, Smurov, I and Grevey, D. (2000), Application of near infrared pyrometry for continuous Nd:YAG laser welding of stainless steel, Applied surface science 168 (2000) 182-185, 2000

Farson, D. (1999), "Laser welding penetration monitoring with multiple emissions signal measurements," Journal of Laser Applications 11(2): 47-53, 1999

Farson, D, and Kim, K, R (1999), "Generation of optical and acoustic emissions in laser weld plues," Jurnal of applied physics, 85(1999), 1329-1336, 1999

Gu, H, P and Duley, W. W. (1996), "Resonant acoustic emission during laser welding of metals," J Phys. D: Appl. Phys. 29 (1996) 550-555.

Jeon, M, Kim, W, Han, G and Na, S. (1998), "A study on heat flow and temperature monitoring in the laser brazing of a pin-to-plate joint," Journal of materials processing technology, 82 (1998) 53-60

Klein, M and Bodenhamer, T, Laser ultrasonics technology report, http://www.industrial-laser.com

Kroos, J., Gratzke, U., Vicanek, M. and Simon, G., (1993) "Dynamic behaviour of the keyhole in laser welding," Journal of Physics, D: Applied Physics, 26, 1993, 481-486

Lankalpall, K. N. T., J. F, and Gartner, M. (1996), "A model for Estimating Penetration Depth of Laser Welding Processes," Journal of Physics: Apply Physics 29(7): 1831-1841, 1996

Li, L, Brookfield, D, J. and Steen W., M. (1996), "Plasma charge sensor for in-process, non-contact monitoring of the laser welding process," Meas, Sci, Technol. 7 (1996), 615-626.

Li, L. (2002), "A comparative study of ultrasound emission characteristics in laser processing," Applied surface science, 186 (2002): 604-610

Lim, D, Cho, Y, Gweon, D. (1998), "A robust in-process monitoring of pulsed laser spot welding using a point infrared sensor," Proceedings of the Institution of Mechanical Engineers, Part B, Engineering Manufacture, Vol. 212, Issue 3, 241-250, 1998.

Liu, Y. S. and Li, X. Y. (2002), "Decentralized robust adaptive control of nonlinear systems with unmodeled dynamics," IEEE Transactions on Automatic Control 47(5): 848-856, 2002

Liu, Y. S., and Li, X. Y. (2003), "Robust adaptive control of nonlinear systems represented by input-output models," IEEE Transactions on Automatic Control 48(6): 1041-1045, 2003

Liu, Y. S., and Li, X. Y. (2004), "Robust adaptive control of nonlinear systems with unmodeled dynamis," IEE Proceedings-Control Theory and Applications 15151(1): 83-88, 2004

Migliore, L. (1998), "Welding with Lasers," Industrial Laser Review, 1998

Miller, M, Mi, B, Kita, A and Ume, C. (2002), "Development of automated real-time data acquisition system for robotic weld quality monitoring, Mechatronics, 12 (2002), 1259-1269

Morgan, S. A. F., M D T; McLean, M A; Hand, D P; Haran, F M; Su, D; Steen, W M; Jones, J D C. (1997), "Real-time process control in CO2 laser welding and direct casting: focus and temperature," ICALEO '97: Laser Materials Processing. San Diego, California; USA. 83: G290-G299, 1990

Na, X. D., Zhang, Y. M., Liu, Y. S. and Walcott, B. (2009), "Nonlinear Identification of Laser Welding Process," IEEE Transactions on Control Systems Technology, Digital Object Identifier 10.1108/TCST.2009.2026163

Park, H and Rhee, S. (1999) "Estimation of weld bead size in CO2 laser welding by using multiple regression and neural network," Journal of Laser Applications 11(3): 143-150, 1999

Park, H and Rhee, S. (1999), "Analysis of mechanism of plasma and spatter in CO2 laser welding of galvanized steel," 31 (1999) 119-126

Park, Y, W, Park, H, Rhee, S and Kang, M. (2002), "Real time estimation of CO2 laser weld quality for automotive industry," Optics & laser Technology 34 (2002) 135-142.

Pedrotti, F. L. a. P., L.S. (1993), "Introduction to Optics," New Jersey, Prentice Hall, 1993

Ono, M, Nakada, K and Kosuge, S, An investigation on CO2 laser-induced plasma, J Jpn Weld Soc, 10(1992): 239-245

Ostendorf, A, Specker, W, Stallmach, M and Zeadan, J. (2003), "3D-MID and process monitoring for micro joining applications," Proceedings of the society of photo-optical instrumentation engineers (SPIE) 4977, 508-517, 2003

Ostendorf, A, Kulik, C, Stallmach, M and Zeadan, J. (2004), "Basic investigations for controlling the laser spot welding process when packaging 3-dimensional molded interconnect devices," Proceedings of the society of photo-optical instrumentation engineers (SPIE) 5339, 441-447, 2004.

Ostendorf, A. and Temme, T. (2004), "Laser spot welding of electronic micro parts," Proceedings of the society of photo-optical instrumentation engineers (SPIE) 5662, 306-312, 2004.

Sforza, P and Blasiis, D. (2002), "On-line optical monitoring system for arc welding," NDT&E international 35 (2002) 37-43

Shao, J and Yan, Y. (2005), "Review of techniques for On-line Monitoring and Inspection of Laser Welding," Journal of Physics: Conference Series 15 (2005), pp. 101-107, 2005

Steen, W, M and Weerasinghe, W, M, Monitoring of laser material processes, SPIE Proc. 650(1986), 160-166.

Sun, A., Kannatey-Asibu, Jr. E. (1999), "Sensor systems for real-time monitoring of laser weld quality," Journal of Laser Applications 11(4): 153-168, 1999

Sun, A., Kannatey-Asibu, Jr. E. (2002), "Monitoring of Laser Weld Penetration Using Sensor Fusion," Journal of Laser Applications 14(2): 114-121, 2002

Sun, Z, Salminen, A. S. and Moisio, T. J. I. (1993), "Quality improvement of laser beam welds by plasma control," Journal of Materials Science Letters, Vol. 12, No. 14, Springer Netherlands, January, 1993

Tonshoff H, K, Ostendorf A, Guttler R, Specker W. (1998), "Online monitoring and closed-loop control of laser welding processes," 12th international symposium for electromachining(ISEM), Aachen, Germany, May 11-13, 1998, 1405 603-612, 1998.

Williams, C. (1997), "CO Laser Processing-An Overview," Aircraft Engineering and Aerospace Technology 69(1): 43-52, 1997

Zhang, X, Chen, W, Ashida, E and Matsuda, F. (2004), "Relationship between weld quality and optical emissions in underwater Nd:YAG laser welding," Opticas and lasers in engineering 41(2004), 717-730

Zhang, Y. M., Kovacevic, R. and Li, L. (1996), "Characterization and real-time measurement of geometrical appearance of the weld pool," Int. J. Mach. Tools Manufact. Vol. 36 No. 7, 799-816, 1996

Laser Welding

Edited by Xiaodong Na, Stone

ISBN 978-953-307-129-9

Hard cover, 240 pages

Publisher Sciyo

Published online 17, August, 2010

Published in print edition August, 2010

This book is entitled to laser welding processes. The objective is to introduce relatively established methodologies and techniques which have been studied, developed and applied either in industries or researches. State-of-the art developments aimed at improving or next generation technologies will be presented covering topics such as monitoring, modelling, control, and industrial application. This book is to provide effective solutions to various applications for field engineers and researchers who are interested in laser material processing.

InTech Europe

University Campus STeP Ri
Slavka Krautzeka 83/A
51000 Rijeka, Croatia
Phone: +385 (51) 770 447
Fax: +385 (51) 686 166
www.intechopen.com

InTech China

Unit 405, Office Block, Hotel Equatorial Shanghai
No.65, Yan An Road (West), Shanghai, 200040, China
中国上海市延安西路65号上海国际贵都大饭店办公楼405单元
Phone: +86-21-62489820
Fax: +86-21-62489821

IntechOpen